diversity

MDPI

Article

Beyond the Beach: Multi-Parameter Interpretation of Shore Deterioration in a Caribbean Reef System

Laura R. de Almeida [1,*], S. Valery Ávila-Mosqueda [2], Edgar Mendoza [1], Brigitta I. van Tussenbroek [2] and Rodolfo Silva [1,*]

[1] Instituto de Ingeniería, Universidad Nacional Autónoma de México, Mexico City 04510, Mexico; emendozab@iingen.unam.mx

[2] Unidad Académica de Sistemas Arrecifales, Instituto de Ciencias del Mar y Limnología, Universidad Nacional Autónoma de México, Puerto Morelos 77580, Mexico; valeryam@ciencias.unam.mx (S.V.Á.-M.); vantuss@cmarl.unam.mx (B.I.v.T.)

* Correspondence: lribasa@iingen.unam.mx (L.R.d.A.); rsilvac@iingen.unam.mx (R.S.)

Abstract: Throughout the Caribbean region, coastal areas are of vital importance for national incomes from the tourism industry. However, accelerated coastal development has impacted the coastal ecosystems, including the beaches, and deterioration of the shore results from cumulative impacts on both marine and coastal ecosystems. It is essential to identify the areas that need special attention for targeted management plans and actions, especially in areas with high anthropogenic pressure. This research proposes an integrated assessment of the conservation state of shore and coastal ecosystems in the Puerto Morelos National Reef Park (PNAPM) in the Mexican Caribbean, through the spatial monitoring of key parameters. A Geographic Information System (GIS) was employed to analyze the land use on the shore, foredune condition, morphological characteristics of the beaches, shoreline evolution, and the condition of coral reefs and seagrass meadows. The analysis identified the most critical areas in relation to shore deterioration and priority areas for the preservation of ecosystems. The spatial data obtained for the PNAPM can serve as a basis for ongoing shore monitoring, and targeted management actions through the designation of areas that require either preservation or ecosystem restoration practices. This methodology can be applied to other reef systems in the Caribbean.

Keywords: coastal ecosystems; coastal management; shore condition; monitoring; critical areas; foredune; beach; seagrass meadow; coral reef

Citation: de Almeida, L.R.; Ávila-Mosqueda, S.V.; Mendoza, E.; van Tussenbroek, B.I.; Silva, R. Beyond the Beach: Multi-Parameter Interpretation of Shore Deterioration in a Caribbean Reef System. *Diversity* **2024**, *16*, 266. https://doi.org/10.3390/d16050266

Academic Editor: Marlenne Manzano-Sarabia

Received: 27 March 2024
Revised: 19 April 2024
Accepted: 26 April 2024
Published: 30 April 2024

1. Introduction

Caribbean coastal areas are amongst the most important global tourist destinations, mainly due to their good climate, white sandy beaches, and clear waters [1]. However, several disturbances, such as sea level rise, increase in water temperature, algal blooms, anthropogenic eutrophication, and the inadequate occupation and use of coastal areas, have caused environmental degradation, including shoreline erosion, decreased water transparency, and the deterioration or destruction of coastal ecosystems [2–6].

The sandy shores, referred to in this article as the active littoral zone, include foredunes, beach and surf zones, and are highly valued as sites of recreation [7]. These shores, at the land–sea interface, are highly dynamic environments, and the characteristics of sediment, tide, currents, wind, and wave climate, together with the characteristics of adjacent ecosystems, define their morphologies [8]. These areas provide important ecosystem services such as coastal flood protection, erosion control, and coastal stabilization, mainly against extreme events and climate change processes [7,9].

In the Caribbean, the shore is often part of a reef system of interconnected ecosystems that includes foredunes, sandy beaches, seagrass meadows, and coral reefs [10,11]. Coral reefs dissipate the incident wave energy from the open sea, favoring the development of

seagrass meadows in calmer waters, which in turn support the existence of the reefs as they improve the water quality [12]. Seagrass canopies also dissipate wave and current energy and their structural characteristics, together with those of coral reefs, influence the morphodynamics of the shore [10,13,14]. The loss of coastal dunes and seagrass meadows, which both accumulate and stabilize sediments, alters sediment transport pathways [15]. Therefore, any change in either one of these ecosystems affects the others. This poses a difficulty in understanding shore morphology dynamics, as the internal positive and negative feedback loops within and between ecosystems are context-dependent, and they often cause non-linear responses, delay, or bi-stability [16–19].

For the coasts of the Caribbean reef systems, there are a number of parameters that can be used to indicate the shore deterioration/conservation condition. The simplest is probably the land use on the shore, including the identification of stretches with severe beach erosion, which can be obtained through visual inspection. Information concerning the deterioration/conservation condition, height, and area of the foredunes provides valuable insight into their ability to protect the coast from flooding [20–22]. Additional methods of assessing the condition of the sandy shore include analyzing sediments, beach profiles, and shoreline evolution. A grain size analysis can help in explaining beach dynamics, as it reflects the dynamics of erosion, transport, and deposition, especially in the swash zone [8]. Beach profile surveys, carried out along the shore, provide important information about spatial variation in the morphology of the beach and foredune, when present; if they are repeated at appropriate time intervals, they may provide details on the magnitude and frequency of cross-shore and shoreline position changes [23]. In the absence of previous beach profile information, the analysis of historical satellite imagery may offer an adequate substitute for defining shoreline evolution, data extremely useful for quantifying historical erosion/accretion rates [24]. Key parameters used as indicators of the conservation state of the coast should also include spatial and temporal data about adjacent marine ecosystems, such as seagrass beds or coral reefs, due to their relationship and connectivity with the shore [10,14,25].

Most studies conducted in the Caribbean evaluated parameters on coastal ecosystems and on the shore separately [5,26–30]. Identification of the main problem of a shore using key parameters and an integrated analysis of them would enable a better understanding of the entire coastal environment, diagnosis of the shore, and identification of critical areas in terms of shore deterioration. The use of a Geographic Information System (GIS) to visualize and analyze the spatial data of such key parameters facilitates the interpretation of results and practical implementation for coastal management.

This work applies such an analysis for Puerto Morelos National Reef Park (Parque Nacional Arrecife de Puerto Morelos, PNAPM in Spanish) in the Mexican Caribbean, an area of great ecological and economic importance [30,31] but one that has faced high anthropogenic pressure, and erosion issues, as verified by [32,33].

The aim of this study was to apply GIS maps of multi-parameter analysis of the shore and adjacent coastal ecosystems that can, together, indicate the condition of the PNAPM (foredune–beach–seagrass meadows–coral reef system) to determine the spatial distribution of shore problems, to identify areas that need special attention due to shore deterioration, and for conservation purposes.

2. Study Area

The Puerto Morelos National Reef Park (PNAPM), in the northern Mexican Caribbean, encompasses 9066 hectares, extending 21 km alongshore and 4–5 km from the shore towards the sea (Figure 1). It includes the shore, a reef lagoon mainly covered by seagrass meadows, and a fringing coral reef that runs parallel to the shore and, further offshore, a portion of the continental shelf area, extending to the depth of 25–30 m. It was declared a marine protected area (MPA) in 1998 with the aim to safeguard the natural heritage of coral reefs and coastal ecosystems, which are important resources for the local community and tourism [30,31].

Since that date, there has been a considerable increase in tourist activities: from ~400 hotel rooms in 1998 to ~7200 rooms in 2023 [34,35].

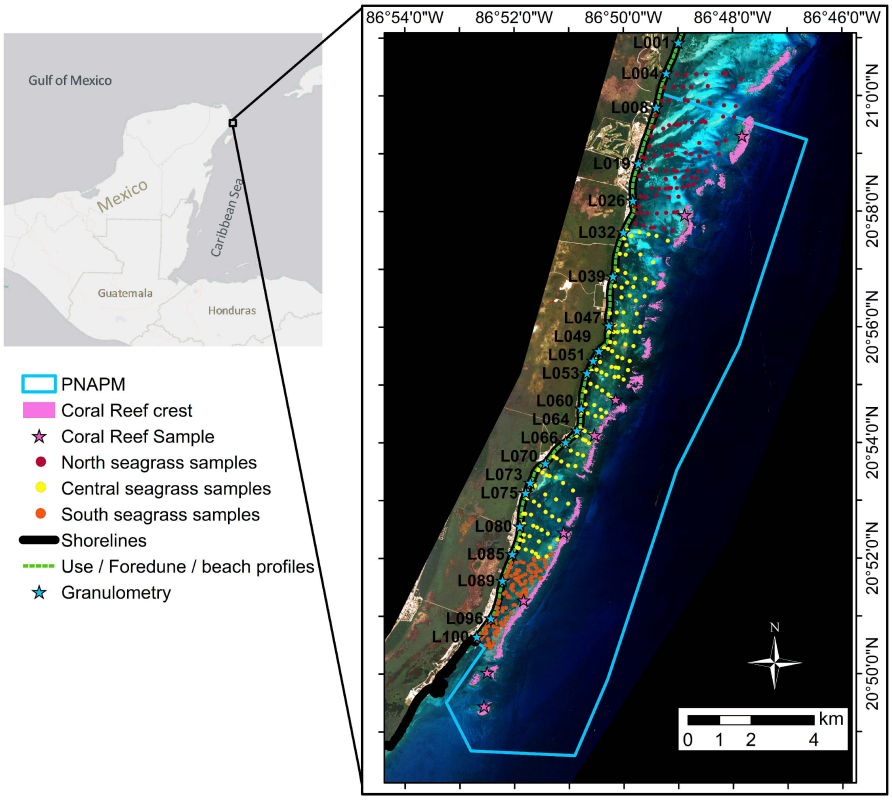

Figure 1. Puerto Morelos National Reef Park (PNAPM) with locations of each data group shown.

The area has a microtidal regime, with spring and neap tidal ranges of 0.32 m and 0.07 m, respectively, and a mean tidal range of ~0.17 m [36]. The shore of the PNAPM generally runs NNE to SSW, perpendicular to 90% of the incident waves, from the E and SE. The significant wave height (Hs) ranges from 0.5 to 1.5 m with mean wave periods (Tm) of 4 to 6 s. In winter (November to April), cold fronts generate energetic, northerly waves (Hs of 2–3 m and Tm of 6–8 s) [14,36]. From June to October, tropical cyclones and hurricanes occasionally generate large waves (Hs of 6–15 m; Tm of 8–12 s) [37].

During the period of analysis (2011–2023), the PNAPM coast was not hit by any category 4 or 5 hurricanes, such as those of 1988, Gilberto, and 2005, Wilma, which significantly affected the biota and the coastal zone [37–39]. Less powerful hurricanes (category 1 and 2) made landfall on the NE coast of Quintana Roo, crossing relatively quickly (1 to 2 h), in October 2020, Delta and Zeta, and August 2023, Grace, using data from [40], with no important damages noted on the coast.

The PNAPM coastline is protected by a fringing coral reef which dissipates up to 85% of the incident wave energy through the friction exerted by bottom rugosity [14]. The level of protection varies depending on the morphology of the reef and its distance from the shore, ranging from 500 to 3000 m. The coral reef of the PNAPM is not continuous along the coast, as it is interrupted by channels that connect the reef lagoon and the offshore ocean [36]. Maximum protection is provided in sections where the back-reef is well developed and the crest is very shallow [20].

The reef lagoon has an average depth of 3–4 m and maximum depth of 8 m. Most of the bottom is covered by calcareous sand, stabilized by mixed seagrass meadows dominated by the species *Thalassia testudinum* and *Syringodium filiforme*, and, to a lesser extent, *Halodule wrightii*, in association with rhizophytic algae [26].

Despite the multiple, valuable services provided by the ecosystems in the PNAPM, these have been directly affected by various local and global stressors such as seawater

contamination through groundwater pollution [41], coral bleaching and disease events [42], and, since 2014, the recurrent, periodic massive beaching of holopelagic *Sargassum* spp. [6,43]. These stressors have caused changes in the vegetative community of the reef lagoon, including the loss of near-shore seagrasses [6,26] and the loss of key reef-building species, with a consequential decrease in rugosity [38,44,45]. This degradation of ecosystems is signaled as one of the causes of the changes on the shore, such as the erosion of beaches and foredunes [4].

3. Materials and Methods

3.1. Land Use on the Shore

The classification of the shore use was based on visual, in situ inspection (Figure 1), in December 2022, with classes defined by the predominant occupation (description in Table 1 and examples in Figure 2A). The class "Erosion" was included to highlight areas where the action of waves and tides on anthropic structures (houses, walls, or hotels) is no longer buffered by a beach or dune, even under calm hydrodynamic conditions. The survey included a category for "new hotels" to account for the two large hotels under construction at the time of the survey. These hotels may eventually impact the beach characteristics in different ways than those hotels currently operating. The study did not consider different uses for stretches less than 50 m long (e.g., natural spaces between hotels), except in areas where erosion was identified. The boundaries of each stretch were determined using geographic coordinates and a PlanetScope satellite image from 30 November 2022.

Table 1. Classes of land use on the shore.

Classification	Description
N = Natural	In a natural state, without human structures/occupation on the foredunes and beach, but not necessarily untouched (there are cases of human actions or structures just landwards of the foredune).
U = Urban	Occupation by houses, public promenades, small hotels or bars/restaurants.
H = Hotel	Presence of large hotels, occupying >150 m along the shore
HN = Hotel New	Large hotels under construction at the time of evaluation
E = Erosion	Eroded shore, where the sea collides with infrastructure under calm conditions. The backshore (from structures to the mean sea level) < 15 m wide. Subdivided into
EH = Erosion—Hotel	EH = erosion on shore used by large hotels;
EU = Erosion—Urban	EU = erosion on shore with urban use.

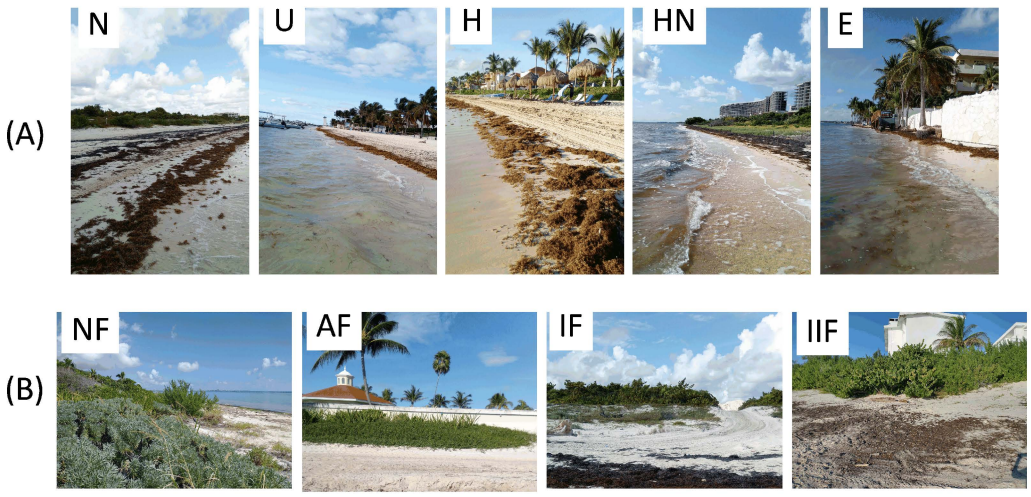

Figure 2. Examples of (**A**) land use on the shore: N = Natural; U = Urban; H = Hotel; HN = Hotel New; E = Erosion; and (**B**) foredune types: NF = natural; AF = artificial; IF = interrupted; IIF = interrupted and impacted (photos L.R. de Almeida).

3.2. Foredune Characterization

The foredunes along the shore (Figure 1) were visually classified in December 2022, based on their naturalness and morphological changes, indicative of the state of the deterioration of the foredune (detailed in the Table 2, with examples in Figure 2B). In this research, the maximum degree of deterioration considered for this ecosystem is the absence of foredunes due to human occupation. This classification was adapted from [13], who verified the state of the foredunes throughout the Mexican Caribbean, and it includes two additional classes: "Artificial Foredunes" and "Interrupted and Impacted Foredunes".

Table 2. Description of foredune types.

Classification	Description
AF = Artificial foredune	Foredunes where morphological conditions were artificially made, favoring or creating an accumulation of sediments where typical dune vegetation developed. Indicates high deterioration of the foredune
NF = Natural foredune	Foredunes in natural morphological conditions (the dune is in an area without human occupation and the back of the foredune is occupied by natural vegetation). Indicates no deterioration of the foredune
IF = Interrupted foredune	Foredunes interrupted by human-made infrastructure, roads at the back of the foredune, walking trails and/or affected by trampling. Indicates minimal deterioration of the foredune
IIF = Interrupted and impacted foredunes	Foredunes interrupted, and with a very high degree of impact, because they were narrow, or small in area (i.e., highly fragmented). Indicates high deterioration of the foredune.

The height of the foredune (above local mean sea level—MSL) was measured using a differential GNSS (Global Navigation Satellite System—GNSSdif) ComNav N5 RTK, and the location data were corrected, using the INEGI fix GNSS station at Chetumal, Quintana Roo [46], with vertical and horizontal accuracies of a few centimeters and millimeters, respectively.

The foredune areas were estimated through GIS photo-interpretation analysis using (i) ArcGIS Map Service World Imagery [47] from 4 April 2022 (Source Maxar, 0.31 m resolution) and from 9 April 2022 (Source Maxar, 0.5 m resolution); (ii) Planet Scope Ortho Scene from 30 November 2022 (3 m resolution) and SkySat from 26 November 2021 (0.5 m resolution); and (iii) local measurement with a GNSSdif (ComNav N5 RTK). A land use and vegetation map [48] was used as a reference for the back-dune definition.

3.3. Beach Profiles

Beach profiles were measured at 100 cross-sectional transects along the shore (Figure 1), with a distance of ~200 m between them, between November 2022 and February 2023. The data were collected using differential GNSS, from the foredune crest or the beginning of human structures, depending on the use of the shore, to the surf zone (~1 m deep).

The parameters evaluated for beach profiles were backshore width (distance from the mean sea level, MSL, to the crest of the foredune or human-made structure); backshore volume (sand volume between the MSL and the crest of the foredune or human-made structure per meter of shoreline); and the slope of the dry beach, swash zone, and surf zone. The zones were manually delineated by examining changes in the profile slopes, considering the dry beach to be from the seaward side of the foredune toe or human-made structure to ~0.3/0.5 m MSL, the swash zone, from ~0.3/0.5 m MSL to ~−0.15/−0.4 m MSL, and the surf zone, from −0.15/−0.4 m towards the sea to ~−1 m MSL.

3.4. Grain Size Analysis

To evaluate the granulometry of the sediment, samples with approximately 500 g of superficial sand were taken at 22 locations (Figure 1) between November 2022 and February 2023. Sediment was collected from the swash zone at each location, and at 10 of these points, additional samples were taken from the dry beach and the surf zone (~0.5 m depth). The samples were dried in a laboratory oven (40–60 °C), and 150 g was used for analysis.

The grain distribution was carried out using a series of sieves, with mesh openings of 1, 0.8, 0.63, 0.5, 0.4, 0.315, 0.25, 0.125, 0.08, and 0.063 mm. Each sample was shaken at a constant speed for 15 min, and the amount of sand retained by each sieve was weighed using an electronic scale. Granulometric calculations were carried out using the standard procedure described in [49]. From the construction of the granulometric curve, the 50th percentiles (D50) were calculated from the 50% intersection of the curve.

3.5. Shoreline Evolution

To detect changes in shoreline positions from January 2011 to November 2022, 27 satellite images with zero or near-zero percent of cloud cover were used (2 per year from 2011 and 2020, 3 images for 2021 and 4 images for 2022). The images were orthorectified, with geometric and atmospheric correction [50]. Eleven were obtained from PlanetScope satellites (3 m pixel resolution, from 2017 to 2021), and eleven from RapidEye satellites (5 m pixel resolution, from 2011 to 2016). The shoreline was detected using a pixel-based, supervised classification (SNAP 9.0.0 software, Minimum Distance Classifier), by identifying the intersection between the land and sea classes.

Given the microtidal regime of the area (<1 m), errors due to the tide can be ignored, as confirmed by [25]. Care was also taken to use images showing calm wave conditions, thus avoiding errors caused by storm surge, or wave-induced foam from wave breaking. Some shoreline positions were validated with beach profile data obtained from differential GNSS on similar dates (2018–2019, data from [43]; and 2022).

To evaluate the shoreline accretion/regression, perpendicular transects were defined for the same locations of the beach profiles, with one more defined where a beach profile could not be measured due to restrictions to the beach area (a total of 101 locations). The intersection point of each transect and the shoreline provided the shoreline position per transect, per date evaluated.

The shoreline change rate per transect (m/year) was calculated by applying a linear regression y = a*x in relation to the earliest date (7 January 2011, x = 0) where a = m/year of beach loss (−) or gain (+) for the entire period evaluated, as indicated by [51].

3.6. Seagrass Meadow Classification Maps

In 2021, two field campaigns were conducted to assess the characteristics of the seagrass meadows. The first campaign took place in the northern area, between April and June 2021 (105 points evaluated, details in [26]), while the second was conducted in the central area, from September to November, 2021 (137 points evaluated) (Figure 1). For the southern area, the study in [52] was used (146 points evaluated September 2019–January 2020). At each sampled point, photos were taken using 0.25 × 0.25 m, 0.5 × 0.5 m and 1 × 1 m quadrats.

For each sampled point, a class was assigned, based mainly on the abundance and cover of seagrass, macroalgae, and sediment, estimated through the Braun–Banquet scale [53] and Otsu method [54,55] from photos of quadrats. For the central area, an unsupervised classification (12 classes and K-means cluster analysis) was used to help to define the class of each point sampled. Difficulties encountered in preparing the classification map of the central area are presented in [56], the main one being the difficulty in differentiating meadows dominated by seagrass from those dominated by macroalgae. These classified points, transformed into shapefile polygons of 4–6 pixels, named seed pixels were used as input and validation data for the supervised classification of the satellite images.

The bottom cover classes were adapted from [26], considering vegetation as both seagrass and macroalgae. In the present study, the classes used were as follows:

C1 = dense vegetation, with seagrass or algae covering more than 90% of the bottom, on average; with taller seagrasses, canopy height typically ~20–30 cm.

C2 = medium dense vegetation, with seagrass and/or algae covering 70–80% of the bottom; seagrass canopy height typically ~15 cm high.

C3 = sparse vegetation; with a seagrass/algae bottom cover of around 50% (between 40–70%) and seagrass canopy height typically ~10 cm.

C4 = sediment; the bottom has a very low seagrass or algae coverage; on average, the sediment cover is 95%.

The classification map for each area was generated independently due to the different dates of the field campaigns. Satellite imagery acquired for nearby areas, for dates close to the corresponding collection dates (Table 3), was used to generate the three maps. PlanetScope satellite images were used, with a spatial resolution of 3 × 3 m, orthorectified and radiometrically, sensor, and geometrically corrected [50]. These satellite images underwent pre-processing to remove areas that could produce interference (land, turbid areas, structures, and white caps). Depth Invariant Indices (DIIs) were calculated for water column correction, using the method presented by [57].

Table 3. Satellite images, data, and method for classification/validation used in the seagrass meadow classification maps of each area.

Satellite Image Date	Satellite	Mapped Area	Data for Training and Validation of Supervised Classification	Supervised Classification Algorithm/Software Used
28 January 2020	Planet Scope 4 bands	South	146 Ground truth data sampling points from September 2019 and January 2020 [52]	Maximum Likelihood/ENVI
23 January 2021	Planet Scope 4 bands	North	105 Ground truth data sampling points from April to June 2021 [26]	K-nearest neighbors/SNAP
31 October 2021	Planet Scope 8 bands	Central	137 Ground truth data sampling points from September to November 2021	K-nearest neighbors/SNAP

For each image, a supervised pixel classification was conducted, using 70% of its seed pixels as training vectors (80% for the southern area [52]). The classification algorithm (see Table 3 for specifications) used the satellite image spectral band from 465 to 680 nm and the DII index. To verify the accuracy of the maps, the remaining 30% of seed pixels (20% for the southern area) were used in a ground-truth ROIs module of ENVI 5.3 software to calculate the overall accuracy and Kappa coefficient. Other details are shown in [26,52,56]. By integrating the maps of the three areas, a comprehensive characterization of seagrass coverage throughout the PNAPM for 2020–2021 was possible.

3.7. Coral Reef Rugosity Map

The rugosity index presented by [30] was used to indicate the structural complexity of a coral reef, which is one of the most important parameters that defines the ability of a coral reef to dissipate wave energy [10]. The data were obtained by these authors at eight sites (Figure 1) located in the back-reef zone, at 2 to 5 m depth, during June/July 2019. At each site, the rugosity was determined in ten transects, by dividing the total length of a 3 m chain by the length of the chain in contact with the substrate, and the rugosity index was determined as the mean rugosity in the ten replicates.

The present work expanded the value obtained by [30] to the entire back-reef zone, respecting the lateral discontinuities (channels) of the coral barrier, considering that the neighboring areas of the sites have similar rugosity conditions. The coral coverage map used to extend the rugosity index results is from [58], and the bathymetry data used for identifying the back-reef zone and reef channels are from [59].

3.8. Data Analysis

Possible disparities in beach characteristics and shoreline variations among parameters of shore use and the condition of foredunes were assessed with a non-parametric Kruskal–Wallis test using R version 4.3.2 software. In cases where the tests indicated significant

differences, a post hoc analysis was carried out using the Dunn test with Bonferroni adjustment, thereby allowing for multiple pairwise comparisons.

After analyzing the data of the key parameters, the main problems causing shore deterioration and the possible indicators of a critical situation were defined. To carry out a spatial analysis of the shore and coastal ecosystems, the GIS map of each parameter was plotted side by side, using ArcGIS 10.0 software. This analysis was named multi-parameter interpretation. A color system was defined to facilitate the visualization of the data and identification of areas needing special attention. For the quantitative parameters, 6 classes were used, with a color gradient "red–orange–yellow–light blue–dark blue–green" indicating the condition from critical to good. Color classes of the foredune were as follows: red for a stretch of shoreline without foredune and green for a stretch protected by "Natural" foredunes, while light blue, yellow, and orange indicate, respectively, interrupted, interrupted and impacted, and artificial foredunes. For land use classes, green showed "natural" uses (good condition) and red showed "erosion" conditions (critical condition), while the color of the classes urban and hotel does not indicate a shore condition. Seagrass classes followed [26], with colors varying from green ~ denser/taller meadows to yellow ~ bottom without seagrasses. This color system is intended to facilitate the spatial interpretation of the general condition of the shore and coastal ecosystems, and thus the identification of the areas requiring special attention.

4. Results

4.1. Land Use on the Shore

In December 2022, large hotels (classes H, HN, and EH, see Table 4) occupied 43.4% of the PNAPM shore, while urban structures (classes U and EU) occupied 28.3%. The remaining 28.3% was classified as "Natural" without visible traces of use by humans (Table 4). The "Natural" class of land use was fragmented and mainly located in the central–northern part of the study area (Supplementary Material, Figure S1). The most critical condition, "Erosion", was found on 14.6% of the PNAPM shore (classes EU and EH, see Table 4), frequently occurring between latitudes 20°53′30″ and 20°55′00′, but also in small stretches of the southern part, with urban use (EU), and in the northern part, with hotel use (EH) (Figure S1).

Table 4. Land use on the PNAPM shore: length and percentage of each type of land use.

Classes	Total (m)	%
N = Natural	6099.9	28.3
U = Urban	4472.2	20.8
H = Hotel	6337.3	29.4
HN = Hotel New	1477.4	6.9
EH = Erosion—Hotel	1539.3	7.1
EU = Erosion—Urban	1625.7	7.5
Total	21,551.8	100.0

4.2. Foredune Characterization

In December 2022, 48.5% of the PNAPM shoreline was protected by just over 33.5 ha of foredunes (Table 5). Although the foredunes classified as "Natural" represent almost half (47.3%) of the total foredune area, only 14.4% of the PNAPM shore length is protected by this type of foredune. In general, "Natural" foredunes consisted of larger patches than other types of foredunes, presenting on average 51.3 m^2 of foredune per meter of shoreline (Table 5). The foredunes classified as "Interrupted" also offered a somewhat lower, but still significant, protection (40.8 m^2 of foredune per meter of shoreline) to 11.7% of the PNAPM shore. The lowest foredune area per meter of shoreline was that of foredunes classified as "Interrupted and Impacted" and "Artificial" (respectively, 19.2 and 10.8 m^2/m).

Table 5. Area and shoreline length of each type of foredune in the PNAPM (December 2022).

Foredune Type	Total Area (m^2)	Mean Area (m^2)	Area (%)	Shoreline Length (m)	% in Relation to the Total Shoreline (21,558 m)	Area per Shoreline Length (m^2/m)	Mean Height (min, max) (m)
Artificial	24,470.5	1223.5	7.3	2271.6	10.5	10.8	2.57 (1.2–5.2)
Natural	159,302.4	26,550.4	47.3	3103.4	14.4	51.3	2.05 (1.7–3.0)
Interrupted	102,538.3	12,817.3	30.5	2512.1	11.7	40.8	2.75 (2.0–3.4)
Interrupted and impacted	49,567.4	3540.5	14.8	2577.2	12.0	19.2	2.03 (1.5–3.3)
Total	335,878.7		100.0	10,464	48.6		

The mean height of the "Natural" foredunes was 2.1 m (between 1.7 and 3.0 m). "Interrupted and Impacted" foredunes had similar heights (between 1.5 and 3.3 m; mean= 2.0 m), while "Interrupted" foredunes varied from 2.0 to 3.4 m (mean = 2.7 m). The artificial dunes had a greater variation in height (from 1.2 to 5.2 m MSL) (Table 5; Figure 3; Supplementary Material Figure S2).

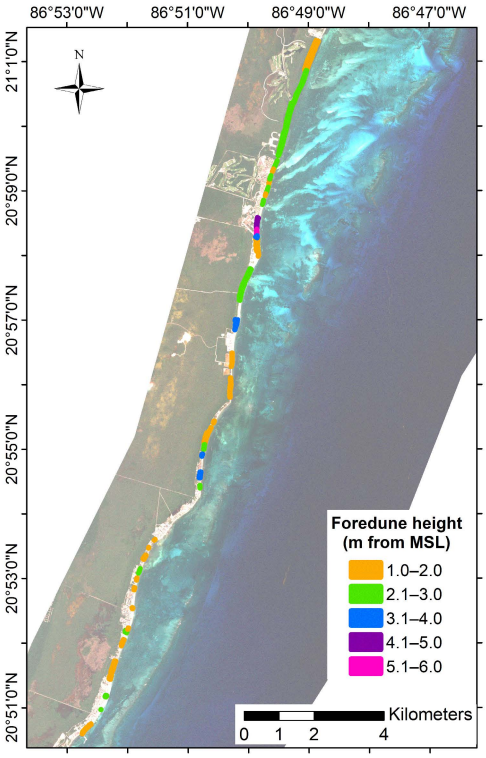

Figure 3. PNAPM foredune heights and locations, December 2022.

The shoreline stretches labeled as "Erosion" lack foredunes, except for one instance where an artificial foredune was constructed in front of an eroded shore used by a hotel. Comparing the land use of the shore where each type of foredune is located (Table 6), "Artificial" foredunes were predominantly located in front of the large hotels, while "Natural" foredunes were only found on shores classified as "Natural", i.e., without human occupation. However, "Natural" shores also had "Interrupted" foredunes, with walking trails or constructions behind the first dune ridges. Foredunes classified as "Interrupted and impacted" were generally found in urban shores (988 m), although the longest length was in front of hotels that were under construction in December 2022 (1442 m). These foredunes may be lost to structures or gardens in the near future, or they may become "Artificial" dunes, if the hotel decides to maintain them as such.

Table 6. Length of shoreline (m) covered by each type of foredune, and the coincidence (in m) of the types of foredune with the land use on the shore.

Foredune Type	Shoreline Length (m)	Coincidence (in m)			
		Land Use on the Shore			
		Hotel	Hotel New	Urban	Natural
Artificial	2271.6	2039	0	77	155 *
Natural	3103.4	0	0	0	3103
Interrupted	2512.1	0	0	112	2400
Interrupted and impacted	2577.2	0	1442	988	148 **
Total	10,464				

* Natural land use, but used to deposit sargassum seaweeds, creating an artificial foredune. ** First line of foredunes adjacent to a plant nursery; the coast was considered natural.

4.3. Beach Profiles

The beach profiles showed a wide range of backshore volumes (1.2–100 m^3/m) and widths (4.7–50.3 m), as well as slopes of dry beach (0.02–0.24), swash (0.07–0.17), and surf zones (0.02–0.37). The slopes did not differ significantly between foredune types (or absence), but a significant difference was verified in the values of backshore volume (chi-squared = 20.4, $p = 0.0004$) and width (chi-squared = 12.2, $p = 0.01$) between profiles without foredunes and profiles with interrupted foredunes (Figure 4A). The shores classified as "Erosion" presented significantly higher dry beach slopes (chi-squared = 25.1, $p = 0.0001$) (except with HN class) and smaller backshore volumes/widths (chi-squared = 38.18, $p < 0.0001$; chi-squared = 35.99, $p < 0.0001$) (Figure 4B; Supplementary Materials Figures S3 and S4).

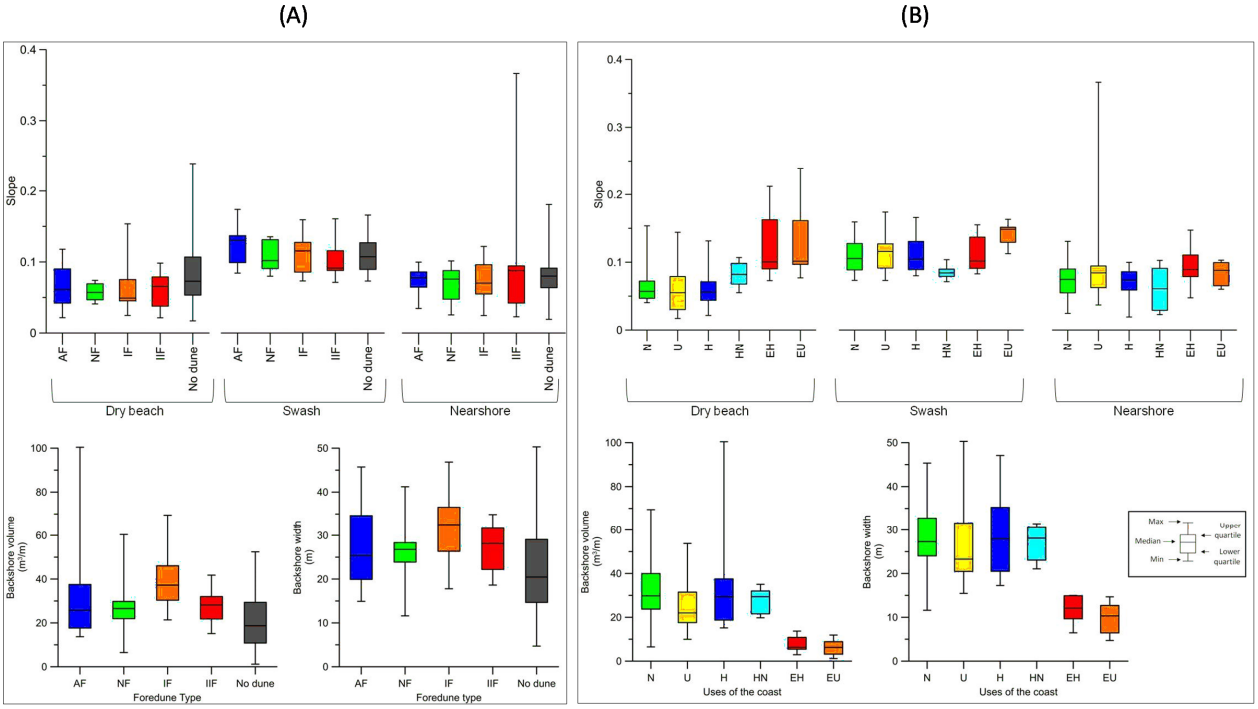

Figure 4. Variations in the characteristics of beach profiles (slopes of dry beach, swash and surf zone; backshore volume, backshore width and slopes), depending on (**A**) foredune type (NF = natural; IF = interrupted; IIF = interrupted and impacted; AF = artificial; No dune), or (**B**) land use on the shore (N = Natural; U = Urban; H = Hotel; HN = Hotel New; EH = Erosion—Hotel; EU = Erosion—Urban).

4.4. Grain Size Analysis

The sediment grain size presented few variations alongshore (Figure 5, Supplementary Material Figure S5) and could be classified as fine-to-medium size, according to scale proposed by [60]. In the swash zone, where most samples were taken, D50 ranged between 0.18 and 0.31 mm (mean 0.23 ± 0.015 mm, 95% confidence interval). Where the sediment size evaluation was made all along the beach profile (dry beach, swash and surf zone, n = 10), the grain size was generally slightly coarser on the dry beach (mean 0.25 ± 0.027) mm than in the swash zone. In the surf zone, D50 presented a greater variation (between 0.18 and 0.49 mm, mean 0.26 ± 0.065 mm, 95% confidence interval). No clear link between grain size and foredune type (chi-squared = 1.05, p = 0.9) was detected. No correlations were observed between grain size and beach profile parameters, the volume and slopes of dry beach, swash, and surf zones (R^2 < 0.2 for all linear regressions).

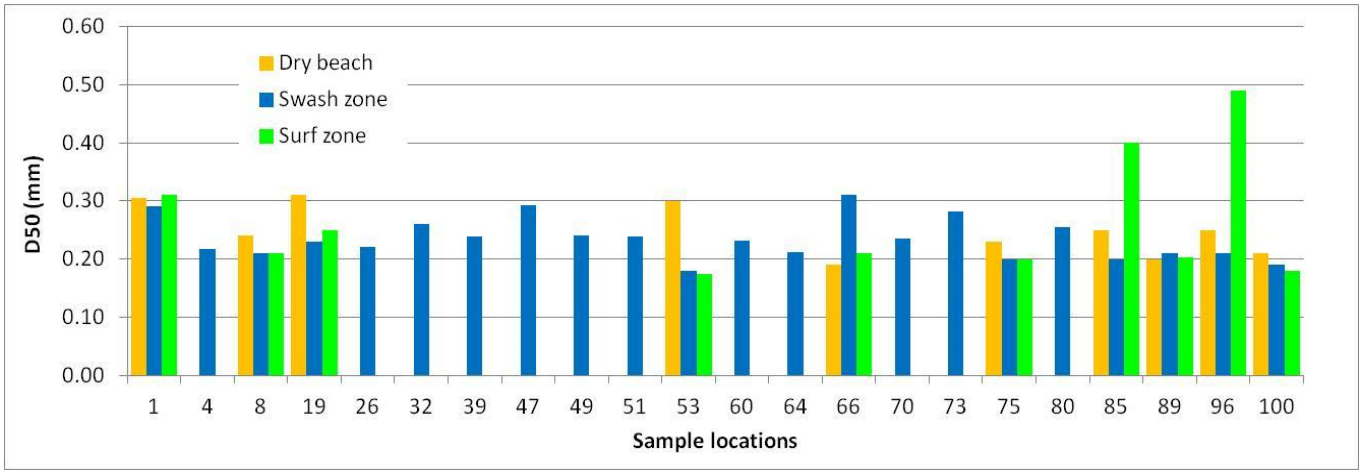

Figure 5. Grain size variation (D50) on the beach profile (dry beach, swash, and surf zone). Sample locations (L) in Figure 1.

4.5. Shoreline Evolution

The shoreline position from the analysis of satellite images showed an average difference equivalent of the size of 1 pixel (3 m) with those from beach profiles (Table 7).

Table 7. Comparison of shoreline positions obtained from satellite images (PlanetScope, pixel resolution of 3 m) and from beach profiles.

Date of Satellite Image (PlanetScope Pixel Resolution of 3 m)	Date of Profiles Measurement	Nº of Beach Profile	Mean (Minimum and Maximum in Parenthesis) Difference between Shoreline Position from Satellite Images and from Beach Profiles (m) *
26 October 2018	3 and 22 October 2018	74	0.7 (−3; 3.4)
5 March 2019	11 February 2019	14	−3.7 (−4.4; −2.9)
23 October 2022	17 and 21 October 2022	10	−2.6 (−4; −1)
30 November 2022	18 November to 13 December 2022	98	−2.9 (−8.6; 2.8)

* Negative values mean that the shoreline is closer to the sea than reality; positive values mean that shoreline is closer to land than reality.

The shoreline change rates (negative = erosion; positive = accretion) showed a general trend of erosion along the entire PNAPM shore from January 2011 until November 2022 (Figure 6, Supplementary Material Figure S6). Most locations (62%) showed shoreline erosion of 1.0–1.9 m/year, and the most severe erosion was 2–3 m/year (at 20% of the locations). Only two locations registered accretional trends: one in the north, where the

hotel's beach management had succeeded in increasing the width of the beach, and the other in the south of PNAPM, where sediment accumulated on the northern side of the breakwater of the Puerto Morelos port.

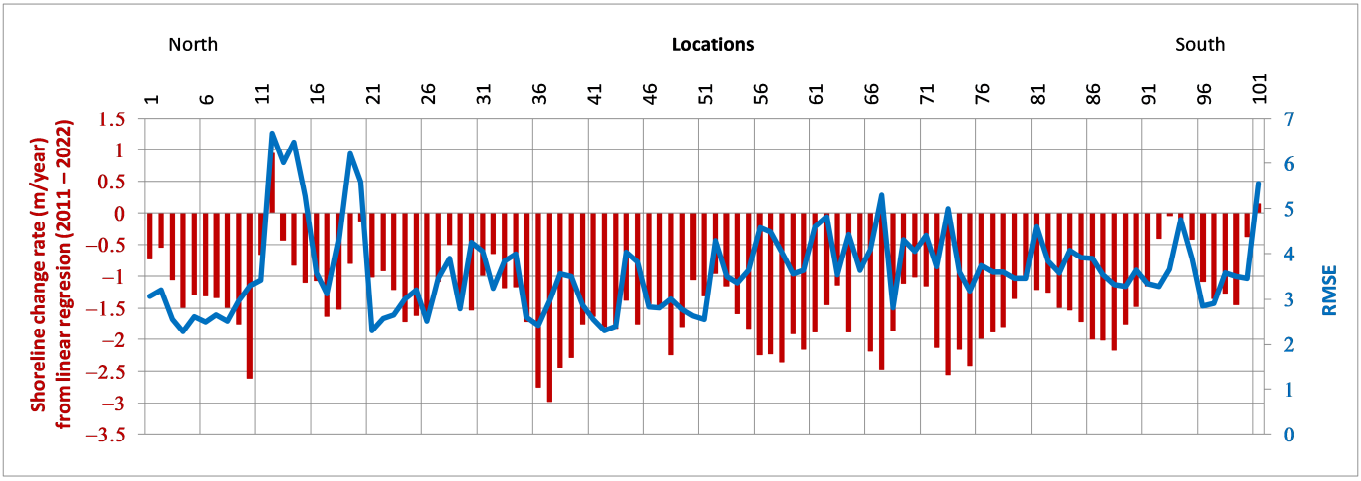

Figure 6. Shoreline change rate (m/year) and the Root-Mean-Squared Error (RMSE) obtained from linear regression of shoreline position between January 2011 and November 2022 (N = 27) in 101 locations of PNAPM shore.

The degree of erosion was independent of foredune type or land use on the shore (Figure 7), except between the EH and U land use (chi-squared = 11.9, p = 0.03). No significant correlations (R^2 < 0.2 for linear regressions) were found between the 2011 to 2022 shoreline change rate and the characteristics of the beach profiles in December 2022 (slope, width, volume, and sediment size).

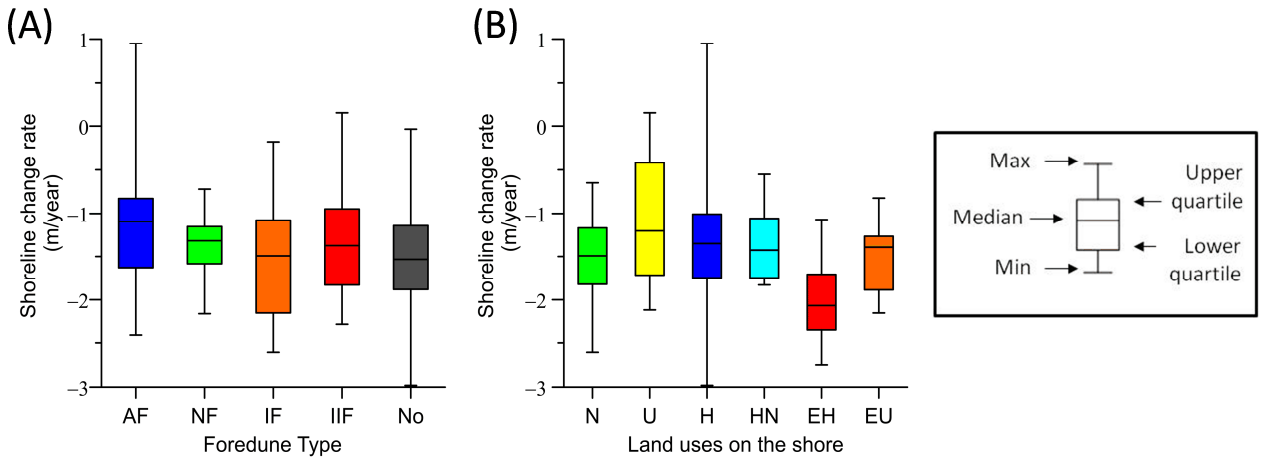

Figure 7. Shoreline change rate (m/year) depending on (**A**) foredune type (NF = natural; IF = interrupted; IIF = interrupted and impacted; AF = artificial; No dune) and (**B**) land use on the shore (N = Natural; U = Urban; H = Hotel; HN = Hotel New; EH = Erosion—Hotel; EU = Erosion—Urban).

4.6. Seagrass Meadow Classification Maps

The maps of the northern, central, and southern reef lagoon areas had an overall accuracy/Kappa index of, respectively, 91%/0.88 [26], 84%/0.78 (present study), and 97%/0.94 [52].

Despite the relatively small size of the study area (<20 km along the shore), important differences were detected among the three areas (Supplementary Material, Figure S7). The northern area had a wider reef lagoon (1.5–3.0 km), with broad C1 class (dense) vegetation. This shore line was less urbanized, with stretches with no visible human occupation (Figure S1). In the first half of 2021, its mixed seagrass meadows showed signs of good health (no epiphytes, and few algae in the meadows), except for the strip closest to the shoreline, which showed signs of impact due to the massive arrival of the holopelagic *Sargassum* spp. causing sargassum brown tides (accumulation of organic matter on the bottom, brown tide/turbid water) [6]. The mean shoreline change rate for this area, for 2011–2022, was −1.1 m/year.

The narrower reef lagoon in the central and southern areas (0.5–1.5 km) was more affected by anthropic activities, with more intensive urban or hotel land uses (Figure S1). In the survey at the end of 2021, signs of seagrass meadow degradation were seen in the central area, where the bottom was dominated by fleshy alga such as *Caulerpa* sp. and *Avrainvillea* sp. or seagrasses with many epiphytes. In this central area, there were few satellite images with clear water for the dates close to the field analysis (August–November 2021). Most images with low cloud cover showed turbid water, mainly due to the sargassum brown tides. It was impossible to map some bottoms, closest to the coast, because of high turbidity [56]. Notwithstanding, a strip of dense vegetation (class C1) was seen near the coast in the central area, with more signals of deterioration (epiphytes and higher participation of opportunistic macroalgae) than in the northern area. The shoreline change rate in this area, for 2011–2022, was usually over 2 m/year erosion, a mean shoreline change rate of −1.7 m/year.

In the southern area of PNAPM, the entire reef lagoon was dominated by class C2 (medium dense vegetation), with small patches of C1 within C2 meadows, and a narrow strip of C1 very close to the coastline. A mean shoreline change rate of −1.1 m/year was recorded for this area.

4.7. Coral Reef Rugosity

According to [30], in 2019 the rugosity index of the PNAPM coral reef varied between 1.28 and 2.08, indicating poor (1.2–1.49), fair (1.5–1.99) and good (2.0–2.5) conditions. The coral reefs with lower rugosity were found in the central section of the PNAPM. The reef with a good rugosity condition was at latitude 20°52′30′′ (Supplementary Material, Figure S8).

4.8. Integrated Multi-Parameter Shore Evaluation

Our results indicate the main reasons for the degradation of the shore in this study area, specifically. These are the erosion of the shore, indicated by the shoreline change rate and "Erosion" class of land use on the shore, the removal or deterioration of the foredunes, and the low values of the backshore volume.

Based on the previous causes and the analysis presented in the previous sections, the four indicators of the most deterioration of the PNAPM shore were defined as (i) "Erosion" as the land use classification of the shore; (ii) absence of foredune; (iii) backshore volume < 10 m^2/m; and (iv) erosion rates >2 m/year.

The multi-parameter map, created through GIS tools, integrates all the available information, and it allows us to make a general spatial description of the state of the PNAPM coast. Critical areas in terms of shore deterioration, where at least two indicators were found, are highlighted by red rectangles in Figure 8.

This assessment also enabled identification of priority areas for shore preservation. These areas were generally located on stretches with no human occupation, adjacent to critical and/or with natural or interrupted foredunes. These preservation priority areas are marked in lilac in Figure 8

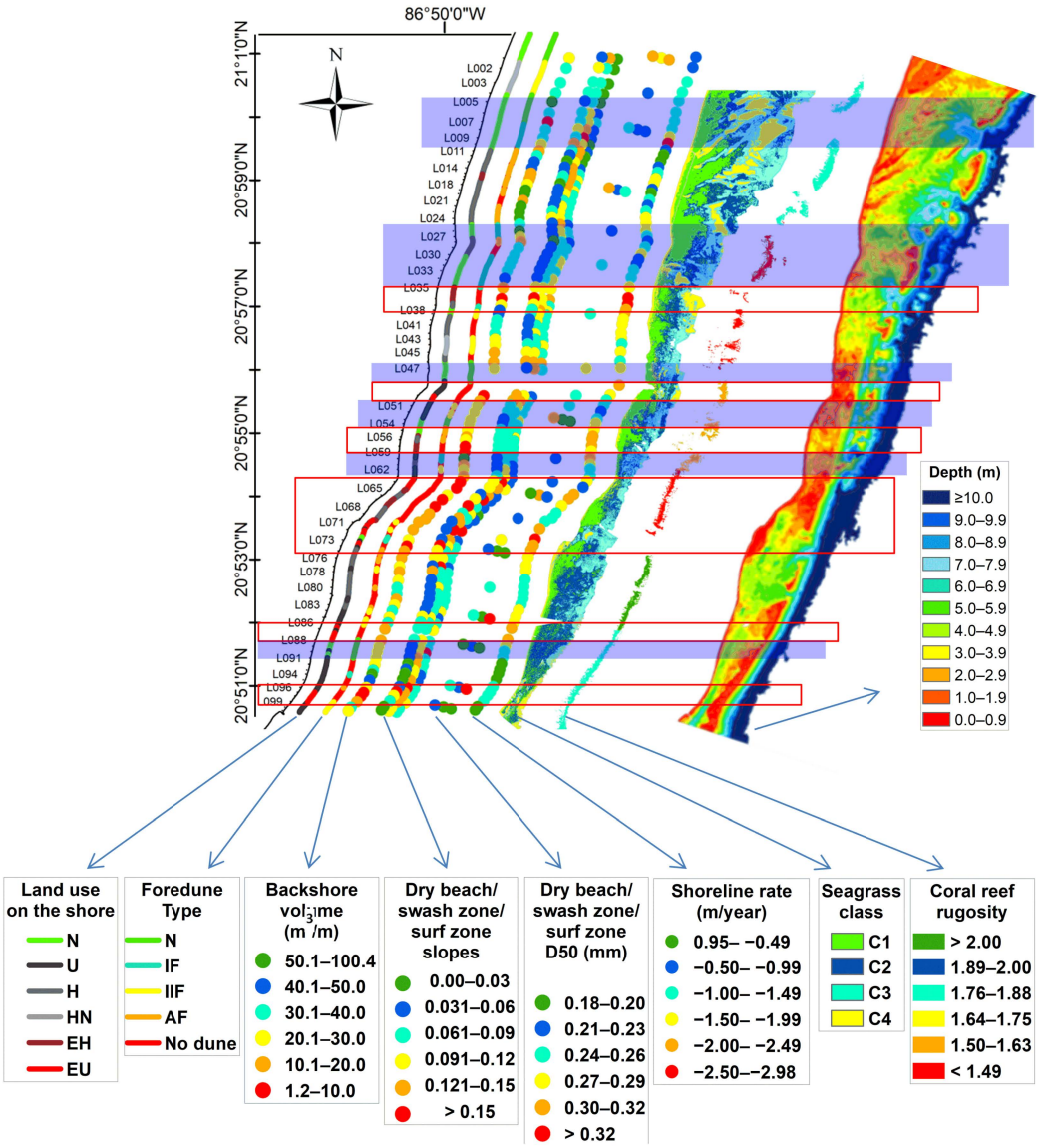

Figure 8. Integrated map of the condition of the shore and coastal ecosystems, indicating the critical areas of the PNAPM shore (red rectangles) and priority preservation areas (marked in lilac), based on data presented in this article. Land use on the shore: N = Natural; U = Urban; H = Hotel; HN = Hotel New; EH = Erosion—Hotel; EU = Erosion—Urban. Foredune Type: NF = natural; IF = interrupted; IIF = interrupted and impacted; AF = artificial. Seagrass class: C1 = dense vegetation; C2 = medium dense vegetation; C3 = Sparse vegetation; C4 = sediment.

5. Discussion and Conclusions

In this study, several key parameters were used to describe the condition of the shore and coastal ecosystems of the PNAPM, and each is discussed below.

The occupation or land use on the shore proved to be a valuable source of information and easy to obtain. It allowed for the identification of actors for Integrated Coastal Zone Management, the degree of anthropization, and the estimation of human-induced pressure. Continuous monitoring of land use on the shore, using the data presented in this work as a starting point, would identify future changes on the shore and make it possible to define the relationship between these changes and the deterioration, or recovery, of the shore. In December 2022, only 28.3% of the PNAPM shore was classified as "natural", with most (43.4%) being used by large hotels. There are social consequences associated with this issue, such as the "gentrification" of beach use, because some hotels do not permit public access to the beaches under their concession. However, the indicator that best evidenced shore

deterioration was the "Erosion" class of land use, identifying stretches where the shore no longer had a dry beach, totaling a considerable 14.6% of the PNAPM shore.

Foredunes are an integral part of the natural dynamics of the beach [61], and their classification indicated the condition of the shore, once their deterioration reduce their protection of the coast against erosion, flooding in extreme events, and climate change [21]. In December 2022, only 38.2% of the PNAPM shore was protected by naturally created foredunes, and approximately one-third of these were highly impacted (Table 5). The importance of foredunes to coastal protection is acknowledged globally [8,21,22], while the alarming loss and degradation of foredunes in PNAPM is evident. Data from [62], [13], and the present study show that there has been an exponential decrease in foredune areas between 2011 and 2022 (Figure 9), resulting in a loss of 63.7% of the foredune area during this period. It is worth noting that several hotels have created artificial dunes in front of their structures, which comprised 10.5% of the PNAPM shoreline length. These artificial foredunes had a much smaller area per meter of shoreline (10.8 m^2/m) compared to the natural foredunes in a relatively good condition (40–50 m^2/m), although some of these artificial foredunes were the highest dunes recorded in the PNAPM. However, they may not be in equilibrium in terms of volume or position, naturally determined by coastal and wind dynamics [63], making them more unstable. In spite of this, these mitigation initiatives do provide some coastal protection against normal events of high wave energy, but they are possibly not effective in protecting the shore during extreme events. Future studies are needed to ascertain the effectiveness of these artificial foredunes in terms of coastal protection.

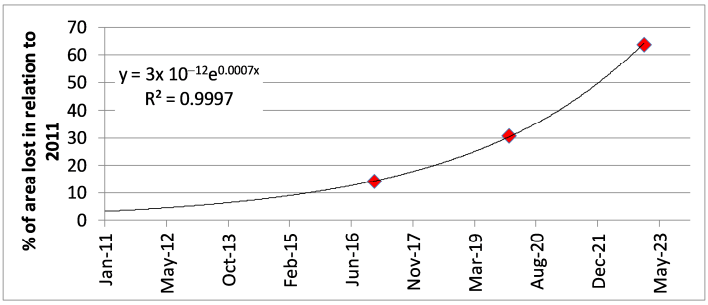

Figure 9. Percentage of foredune area lost in relation to 2011 (2011 and 2017, data from [62]; 2019 data from [13]).

The characteristics of the beaches (backshore volumes and widths, slope value of dry beach, swash and surf zone, and grain size) were not significantly related to neither specific land uses on the shore (except for areas categorized as Erosion), nor the type, or absence, of foredunes. Unfortunately, there has been no continuous beach profiling in the study area to reveal the causes of the changes in beach characteristics. Regular, frequent beach profile monitoring would highlight areas that are losing backshore volume, or where the slope is changing, which would indicate changes in the beach morphodynamics and allow for the plotting of shore evolution in different seasons, or over the years [23]. Such monitoring should be performed at least twice a year (in periods with most and least energy) to identify possible effects that the land uses on the shore, and the foredune type, have on the beach. As beach profile data are crucial for future studies, the data collected for this work are available in the Supplementary Materials, and other researchers may use it as long they cite this publication.

Although the sediment grain size is considered an important factor that defines the shape of a beach profile [64], no relationships were found between grain size and the slope of each beach profile zone, or the volume of the backshore. However, other studies state that the local wave characteristics define the beach profile shape [65,66], and this is possibly the case for the study area. Temporal monitoring of grain size and beach profiles, combined with nearshore wave data, could clarify the effect of sediment and waves on the profile

shape and on beach slopes in the study area. The sediment grain size data obtained in the present study, compared with a few samples from 2007 and 2010 [67], do not show important changes. However, as few sediment samples were obtained in the past, and due to the erosive condition of the area, it is recommended that sediment monitoring be carried out parallel to the beach profile monitoring.

The analysis of shoreline evolution over more than a decade in the PNAPM shows widespread shore recession (mean = 1.4 ± 0.13 m/year), except at two points. The erosional trend of the shoreline is in agreement with the findings of various other studies carried out in stretches of the study area [25,32,33]. In general, the rate of shoreline change did not differ significantly between types of foredunes and land uses on the shore. The data on foredune types and land use on the shore were obtained in December 2022, and the shoreline change-rate data were obtained for the period 2011–2022; therefore, the types of foredune or land use data for December 2022 were not reflected in the shoreline change rate for the last decade. The causes of the erosion may be attributed to the estimated 2.5 mm/year rise in sea level in the PNAPM area [68], and/or the degradation of seagrass and coral reef ecosystems over recent years [4,6,38,44]. The degradation of these ecosystems results in the loss of ecosystem services, such as sediment stabilization and the prevention of coastal erosion and flooding [10,19]. In front of the areas with the highest shoreline erosion rates, around ~20°57′ and 20°53′, the seagrass meadows had the worst conditions and the reefs had the lowest value of coral reef rugosity (see Figure 8).

The PNAPM has a program to monitor the seagrass meadows and coral reefs [69], but monitoring efforts were discontinuous and only covered specific areas. High temporal and spatial resolution in monitoring are important for ecosystems undergoing degradation, such as the seagrass meadows and coral reef in PNAPM, since it is difficult to predict their future trajectories of degradation [17,18] if stressors, such as an increase in sea level, nutrients and/or temperature, coral diseases, or the massive beaching of sargassum, continue. This kind of monitoring is expensive and laborious, requiring specialists for each ecosystem, and in remote sensing, to carry out in situ measurements, determine ecosystem status classes, and create classification maps from satellite images and field data. Even so, monitoring should be carried out every 5 years. Because of the importance of seagrasses in shallow-water coastal dynamics, and the recent loss of seagrass meadows following the massive arrival of sargassum [6], it is advisable to monitor the nearshore area, the 400 m closest to the coast, every 2 years.

From an analysis of the general condition, the shore indicators of shore deterioration were identified. The multi-parameter interpretation allowed us to identify sections of the shore that were in critical condition (marked as red rectangles in Figure 8).

The primary cause of the problems in these areas was the occupation of the shore, which had eliminated the foredunes and decreased the backshore volume, resulting in decreased beach buffering. This reduction in volume disrupted the dynamics of the beach, leading to a sediment deficit, accelerating the already prevalent erosion processes along the coast. The largest critical area was found at latitude 20°54″, lying adjacent to seagrass meadows with signs of deterioration and reefs with a low rugosity index, suggesting that the deterioration of marine ecosystems contributes to the further deterioration of the shore. These areas need special attention due to the higher risk of destruction of structures and flooding of the coast. The identification of these areas is important for coastal managers to define better adaptation strategies and/or protection measures [70]. The multi-parameter interpretation also enabled the identification of areas which could be defined as priority areas for preservation actions and ecosystem-based management strategies, especially for foredunes, but also the other coastal ecosystems (in lilac Figure 8). For example, "Natural foredunes" could be protected from the construction of infrastructure, and "Interrupted foredunes" could be recovered through protection and restoration actions.

To the best of the authors' knowledge, this is the first time that detailed spatial data have been obtained and analyzed for a Caribbean reef system and sandy shore. The

methodology can be applied to other, similar areas, and the data can be used as a possible basis for a continuous shore monitoring program in PNAPM.

Criteria for the definition of the critical stretches of a shore will be site-dependent and differ depending on the main stressors to the coastal system. For the area under study, erosion was prevalent along almost the entire shore. Therefore, the identification of the most critical areas was based on pre-existing issues, such as the absence of a beach and foredunes, low backshore volume, and high shoreline erosion rates. Other issues may be vulnerability to the impact of extreme events, which will require different parameters and criteria.

Considering that reef–seagrass–beach–dune systems, common in the Caribbean, can be greatly affected by changes in hydrodynamics and sediment flow, and that these ecosystems are highly interconnected [4,13], traditional protection measures, such as hard engineering defenses or beach nourishment, can cause major impacts to one, and consequently to all coastal ecosystems. Solutions that are ecosystem-based, like coral reef and seagrass restoration, are recommended for this type of system, in order to maintain or enhance coastal environment resilience and ecosystem services, such as defense against extreme waves, flooding, and erosion [71]. Ecosystem-based defense also has additional benefits, such as an improvement in water quality, carbon sequestration, fishing production, nature conservation, and the creation of recreational spaces [72]. Therefore, restoration projects for seagrass and coral reefs are urgently needed in those areas that are critical in shore deterioration and identified as priorities for preservation.

Supplementary Materials: The following supporting information can be downloaded at: https://www.mdpi.com/article/10.3390/d16050266/s1, (i) Figure S1. Land use on PNAPM shore (December 2022): N = Natural; U = Urban; H = Hotel; HN = Hotel New; EH = Erosion—Hotel; EU = Erosion—Urban. Figure S2. Locations of the foredune areas in PNAPM, January 2023: AF = artificial; NF = natural; IF = interrupted; IIF = interrupted and impacted. Figure S3. Spatial variation of backshore volume (m^3/m) calculated from beach profile data in PNAPM, winter 2022/2023. Figure S4. Spatial variation of slope of each beach profile zone obtained in PNAPM, winter 2022/2023: dry beach, swash zone, and surf zone (dry beach and surf zone data points are offset for better visualization). Figure S5. Grain size variation (D50) on PNAPM shore, winter 2022/2023, for dry beach, swash, and surf zone. Locations with only 1 point refer to swash zone samples. Figure S6. Shoreline change rate (m/year, between 2011 and 2022) for each location analyzed along the PNAPM shore. Figure S7. Map of bottom cover classes (vegetation/sediment) of the PNAPM reef lagoon, 2020/2021: C1 (dense vegetation), C2 (medium dense vegetation), C3 (Low dense vegetation), and C4 (sediment). The bottom cover map of south area is an adaptation of [52]. Figure S8. Map of coral reef rugosity index (sites data from [30] and backreef cover from [58]); (ii), Beach profiles database measured in PNAPM between November 2022 and February 2023.

Author Contributions: L.R.d.A., R.S., E.M. and B.I.v.T. contributed to the conception of the study. L.R.d.A. performed all fieldwork and data analysis. S.V.Á.-M. performed seagrass field work and ran all statistical analyses. L.R.d.A. wrote the first draft of the manuscript. All authors wrote sections of the manuscript, reviewed the manuscript, and read and approved the submitted version. All authors have read and agreed to the published version of the manuscript.

Funding: This research was supported by the CONACYT postdoctoral grant to L.R de Almeida, and funded by the GII-UNAM Project "Sostenibilidad del Caribe mexicano: cambiando debilidades en fortalezas", and RENACE (DGAPA—Dirección General de Asuntos del Personal Académico), under project no. PAPIIT AG100321.

Institutional Review Board Statement: Not applicable.

Data Availability Statement: The authors will share the database supporting this research upon reasonable request.

Acknowledgments: The authors acknowledge the Academic Service for Meteorological and Oceanographic Monitoring (SAMMO) of UNAM, especially Edgar Escalante and Miguel Gómez Reali for technical support in logistics and in the field, and Guadalupe Barba-Santos for technical support in the laboratory. The authors also acknowledge Planet's Education and Research (E&R) Program [73].

Conflicts of Interest: The authors declare no conflicts of interest.

References

1. Gable, F.J. Climate Change Impacts on Caribbean Coastal Areas and Tourism. *J. Coast. Res.* **1997**, *SI 24*, 49–69.
2. Velázquez-Ochoa, R.; Enríquez, S. Environmental Degradation of the Mexican Caribbean Reef Lagoons. *Mar. Pollut. Bull.* **2023**, *191*, 114947. [CrossRef] [PubMed]
3. Chollett, I.; Collin, R.; Bastidas, C.; Cróquer, A.; Gayle, P.M.H.; Jordán-Dahlgren, E.; Koltes, K.; Oxenford, H.; Rodriguez-Ramirez, A.; Weil, E.; et al. Widespread Local Chronic Stressors in Caribbean Coastal Habitats. *PLoS ONE* **2017**, *12*, e0188564. [CrossRef] [PubMed]
4. Gómez, I.; Silva, R.; Lithgow, D.; Rodríguez, J.; Banaszak, A.T.; van Tussenbroek, B. A Review of Disturbances to the Ecosystems of the Mexican Caribbean, Their Causes and Consequences. *J. Mar. Sci. Eng.* **2022**, *10*, 644. [CrossRef]
5. Rangel-Buitrago, N.G.; Anfuso, G.; Williams, A.T. Coastal Erosion along the Caribbean Coast of Colombia: Magnitudes, Causes and Management. *Ocean Coast. Manag.* **2015**, *114*, 129–144. [CrossRef]
6. Van Tussenbroek, B.I.; Hernández Arana, H.A.; Rodríguez-Martínez, R.E.; Espinoza-Avalos, J.; Canizales-Flores, H.M.; González-Godoy, C.E.; Barba-Santos, M.G.; Vega-Zepeda, A.; Collado-Vides, L. Severe Impacts of Brown Tides Caused by Sargassum Spp. on near-Shore Caribbean Seagrass Communities. *Mar. Pollut. Bull.* **2017**, *122*, 272–281. [CrossRef] [PubMed]
7. Harris, L.R.; Defeo, O. Sandy Shore Ecosystem Services, Ecological Infrastructure, and Bundles: New Insights and Perspectives. *Ecosyst. Serv.* **2022**, *57*, 101477. [CrossRef]
8. Davidson-Arnott, R. *Introduction to Coastal Processes & Geomorphology*; Cambridge University Press: Cambridge, UK, 2010; ISBN 978-0-511-69133-1.
9. Barbier, E.B.; Hacker, S.D.; Kennedy, C.; Koch, E.W.; Stier, A.C.; Silliman, B.R. The Value of Estuarine and Coastal Ecosystem Services. *Ecol. Monogr.* **2011**, *81*, 169–193. [CrossRef]
10. Guannel, G.; Arkema, K.; Ruggiero, P.; Verutes, G. The Power of Three: Coral Reefs, Seagrasses and Mangroves Protect Coastal Regions and Increase Their Resilience. *PLoS ONE* **2016**, *11*, e0158094. [CrossRef]
11. Rioja-Nieto, R.; Garza-Pérez, R.; Álvarez-Filip, L.; Ismael, M.-T.; Cecilia, E. The Mexican Caribbean: From Xcalak to Holbox. In *World Seas: An Environmental Evaluation Volume I: Europe, the Americas and West Africa*; Sheppard, C., Ed.; Elsevier: London, UK, 2019; pp. 637–653, ISBN 9780128050682.
12. Moberg, F.; Rönnbäck, P. Ecosystem Services of the Tropical Seascape: Interactions, Substitutions and Restoration. *Ocean Coast. Manag.* **2003**, *46*, 27–46. [CrossRef]
13. De Almeida, L.R.; Silva, R.; Martínez, M.L. The Relationships between Environmental Conditions and Parallel Ecosystems on the Coastal Dunes of the Mexican Caribbean. *Geomorphology* **2022**, *397*, 108006. [CrossRef]
14. De Alegria-Arzaburu, A.R.; Mariño-Tapia, I.; Enriquez, C.; Silva, R.; González-Leija, M. The Role of Fringing Coral Reefs on Beach Morphodynamics. *Geomorphology* **2013**, *198*, 69–83. [CrossRef]
15. Feagin, R.A.; Figlus, J.; Zinnert, J.C.; Sigren, J.; Martínez, M.L.; Silva, R.; Smith, W.K.; Cox, D.; Young, D.R.; Carter, G. Going with the Flow or against the Grain? The Promise of Vegetation for Protecting Beaches, Dunes, and Barrier Islands from Erosion. *Front. Ecol. Environ.* **2015**, *13*, 203–210. [CrossRef]
16. McManus, J.W.; Polsenberg, J.F. Coral-Algal Phase Shifts on Coral Reefs: Ecological and Environmental Aspects. *Prog. Oceanogr.* **2004**, *60*, 263–279. [CrossRef]
17. Scheffer, M.; Carpenter, S.; Foley, J.A.; Folke, C.; Walker, B. Catastrophic Shifts in Ecosystems. *Nature* **2001**, *413*, 591–596. [CrossRef] [PubMed]
18. Van Der Heide, T.; Van Nes, E.H.; Geerling, G.W.; Smolders, A.J.P.; Bouma, T.J.; Van Katwijk, M.M. Positive Feedbacks in Seagrass Ecosystems: Implications for Success in Conservation and Restoration. *Ecosystems* **2007**, *10*, 1311–1322. [CrossRef]
19. Barbier, E.B.; Koch, E.W.; Silliman, B.R.; Hacker, S.D.; Wolanski, E.; Primavera, J.; Granek, E.F.; Polasky, S.; Aswani, S.; Cramer, L.A.; et al. Coastal Ecosystem-Based Management with Nonlinear Ecological Functions and Values. *Science* **2008**, *319–321*, 321–323. [CrossRef] [PubMed]
20. Franklin, G.L.; Torres-Freyermuth, A.; Medellín, G.; Allende-Arandia, M.E.; Gómez, B.; Appendini, C.M. The Role of the Reef-Dune System in Coastal Protection in Puerto Morelos (Mexico). *Nat. Hazards Earth Syst. Sci. Discuss.* **2017**, *18*, 1247–1260. [CrossRef]
21. Taylor, E.B.; Gibeaut, J.C.; Yoskowitz, D.W.; Starek, M.J. Assessment and Monetary Valuation of the Storm Protection Function of Beaches and Foredunes on the Texas Coast. *J. Coast. Res.* **2015**, *31*, 1205–1216. [CrossRef]
22. Williams, A.T.; Alveirinho-Dias, J.; Novo, F.G.; García-Mora, M.R.; Curr, R.; Pereira, A. Integrated Coastal Dune Management: Checklists. *Cont. Shelf Res.* **2001**, *21*, 1937–1960. [CrossRef]
23. Cooper, N.J.; Leggett, D.J.; Lowe, J.P. Beach-Profile Measurement, Theory and Analysis: Practical Guidance and Applied Case Studies. *J. Chart. Inst. Water Environ. Manag.* **2000**, *14*, 79–88. [CrossRef]
24. Jaramillo, C.; Sanchez-Garcia, E.; Jara, M.S.; González, M.; Palomar-Vazquez, J.M. Subpixel Satellite-Derived Shorelines as Valuable Data for Equilibrium Shoreline Evolution Models. *J. Coast. Res.* **2020**, *36*, 1215–1228. [CrossRef]
25. Escudero, M.; Reguero, B.G.; Mendoza, E.; Secaira, F.; Silva, R. Coral Reef Geometry and Hydrodynamics in Beach Erosion Control in North Quintana Roo, Mexico. *Front. Mar. Sci.* **2021**, *8*, 684732. [CrossRef]

26. De Almeida, L.R.; Ávila-Mosqueda, S.V.; Silva, R.; Mendoza, E.; van Tussenbroek, B.I. Mapping the Structure of Mixed Seagrass Meadows in the Mexican Caribbean. *Front. Mar. Sci.* **2022**, *9*, 1063007. [CrossRef]
27. Cambers, G. Caribbean Beach Changes and Climate Change Adaptation. *Aquat. Ecosyst. Health Manag.* **2009**, *12*, 168–176. [CrossRef]
28. Alvarez-Filip, L.; Dulvy, N.K.; Gill, J.A.; Côté, I.M.; Watkinson, A.R. Flattening of Caribbean Coral Reefs: Region-Wide Declines in Architectural Complexity. *Proc. R. Soc. B Biol. Sci.* **2009**, *276*, 3019–3025. [CrossRef]
29. Van Tussenbroek, B.I.; Cortés, J.; Collin, R.; Fonseca, A.C.; Gayle, P.M.H.; Guzmán, H.M.; Jácome, G.E.; Juman, R.; Koltes, K.H.; Oxenford, H.A.; et al. Caribbean-Wide, Long-Term Study of Seagrass Beds Reveals Local Variations, Shifts in Community Structure and Occasional Collapse. *PLoS ONE* **2014**, *9*, e90600. [CrossRef] [PubMed]
30. Caballero-Aragón, H.; Perera-Valderrama, S.; Cerdeira-Estrada, S.; Martell-Dubois, R.; Rosique-de la Cruz, L.; Álvarez-Filip, L.; Pérez-Cervantes, E.; Estrada-Saldívar, N.; Ressl, R. Puerto Morelos Coral Reefs, Their Current State and Classification by a Scoring System. *Diversity* **2020**, *12*, 272. [CrossRef]
31. Instituto Nacional de Ecología. *Programa De Manejo Parque Nacional Arrecife de Puerto Morelos, México*. SEMARNAP 2000, 224. Available online: https://simec.conanp.gob.mx/pdf_libro_pm/83_libro_pm.pdf (accessed on 15 May 2022).
32. Valderrama-Landeros, L.H.; Martell-Dubois, R.; Ressl, R.; Silva-Casarín, R.; Cruz-Ramírez, C.J.; Muñoz-Pérez, J.J. Dynamics of Coastline Changes in Mexico. *J. Geogr. Sci.* **2019**, *29*, 1637–1654. [CrossRef]
33. SECTUR. Vulnerabilidad Del Destino Turístico Riviera Maya. In *Estudio de Vulnerabilidad y Programa de Adaptación ante la Variabilidad Climática y el Cambio Climático en dies Destinos Turísticos Estratégicos, así Como Propuesta de un Sistema de Alerta Temprana a eventos Hidrometereológicos Extremos*; Fondo Sectorial CONACYT-SECTUR, Ed.; Academia Nacional de Investigación y Desarrollo A.C.: Cuernavaca, Morelos, Mexico, 2013; pp. 1–39.
34. INEGI Cuartos y Unidades de Hospedaje Registrados Por Municipio Según Categoría Turística Del Establecimiento. Available online: www.inegi.org.mx (accessed on 16 January 2024).
35. Ayuntamiento de Puerto Morelos Ocupaciòn Hotelera de Puerto Morelos Registra Un Crecimiento Sostenido. Available online: https://puertomorelos.gob.mx/comunicacionsocial/ocupacion-hotelera-de-puerto-morelos-registra-un-crecimiento-sostenido/ (accessed on 16 January 2024).
36. Coronado, C.; Candela, J.; Iglesias-Prieto, R.; Sheinbaum, J.; López, M.; Ocampo-Torres, F.J. On the Circulation in the Puerto Morelos Fringing Reef Lagoon. *Coral Reefs* **2007**, *26*, 149–163. [CrossRef]
37. Mariño-Tapia, I.; Enriquez, C.; Silva, R.; Mendoza-Baldwin, E.; Escalante-Mancera, E.; Ruiz-Renteria, F. Comparative Morphodynamics between Exposed and Reef Protected Beaches under Hurrricane Conditions. *Coast. Eng. Proc.* **2014**, *1*, 55. [CrossRef]
38. Estrada-Saldívar, N.; Jordán-Dalhgren, E.; Rodríguez-Martínez, R.E.; Perry, C.; Alvarez-Filip, L. Functional Consequences of the Long-Term Decline of Reef-Building Corals in the Caribbean: Evidence of across-Reef Functional Convergence. *R. Soc. Open Sci.* **2019**, *6*, 190298. [CrossRef]
39. Van Tussenbroek, B.I. The Impact of Hurricane Gilbert on the Vegetative Development of Thalassia Testudinum in Puerto Morelos Coral Reef Lagoon, Mexico: A Retrospective Study. *Bot. Mar.* **1994**, *37*, 421–428. [CrossRef]
40. NOAA National Hurricane Center—Atlantic Hurricane Season. Available online: https://www.nhc.noaa.gov/data/tcr/ (accessed on 8 August 2023).
41. Hernández-Terrones, L.; Rebolledo-Vieyra, M.; Merino-Ibarra, M.; Soto, M.; Le-Cossec, A.; Monroy-Ríos, E. Groundwater Pollution in a Karstic Region (NE Yucatan): Baseline Nutrient Content and Flux to Coastal Ecosystems. *Water. Air. Soil Pollut.* **2011**, *218*, 517–528. [CrossRef]
42. Alvarez-Filip, L.; Estrada-Saldívar, N.; Pérez-Cervantes, E.; Molina-Hernández, A.; González-Barrios, F.J. A Rapid Spread of the Stony Coral Tissue Loss Disease Outbreak in the Mexican Caribbean. *PeerJ* **2019**, *7*, e8069. [CrossRef] [PubMed]
43. Chávez, V.; Uribe-Martínez, A.; Cuevas, E.; Rodríguez-Martínez, R.E.; van Tussenbroek, B.I.; Francisco, V.; Estévez, M.; Celis, L.B.; Monroy-Velázquez, L.V.; Leal-Bautista, R.; et al. Massive Influx of Pelagic Sargassum Spp. on the Coasts of the Mexican Caribbean 2014–2020: Challenges and Opportunities. *Water* **2020**, *12*, 2908. [CrossRef]
44. Alvarez-Filip, L.; González-Barrios, F.J.; Pérez-Cervantes, E.; Molina-Hernández, A.; Estrada-Saldívar, N. Stony Coral Tissue Loss Disease Decimated Caribbean Coral Populations and Reshaped Reef Functionality. *Commun. Biol.* **2022**, *5*, 440. [CrossRef] [PubMed]
45. Rosado-Torres, A.A.; Mariño-Tapia, I.; Acevedo-Ramírez, C. Decreased Roughness and Macroalgae Dominance in a Coral Reef Environment with Strong Influence of Submarine Groundwater Discharges. *J. Coast. Res.* **2019**, *92*, 13. [CrossRef]
46. INEGI Red Geodésica Nacional Activa. Available online: https://www.inegi.org.mx/app/geo2/rgna/ (accessed on 1 January 2023).
47. ESRI World Imagery. Available online: https://www.arcgis.com/home/item.html?id=10df2279f9684e4a9f6a7f08febac2a9 (accessed on 1 March 2023).
48. CONABIO Mapa de Uso Del Suelo y Vegetación de La Zona Costera Asociada a Los Manglares, Región Península de Yucatán. 2015. Available online: http://geoportal.conabio.gob.mx/metadatos/doc/html/py_oc2015gw.html (accessed on 4 February 2021).
49. *ASTM D 422-63*; Standard Test Method for Particle-Size Analysis of Soils. ASTM International: West Conshohocken, PA, USA, 2007.

50. Planet Labs Inc Planet Imagery Products Specifications 2022. Available online: https://assets.planet.com/docs/Planet_Combined_Imagery_Product_Specs_letter_screen.pdf (accessed on 1 June 2022).
51. Luijendijk, A.; Hagenaars, G.; Ranasinghe, R.; Baart, F.; Donchyts, G.; Aarninkhof, S. The State of the World's Beaches. *Sci. Rep.* **2018**, *8*, 6641. [CrossRef]
52. Ávila-Mosqueda, S.V. Variabilidad Espacial En Comunidades de Pastos Marinos Asociada a Afluencias Masivas de Sargassum Spp. Master's Thesis, Instituto de Ciencias del Mar y Limnología, UNAM, Puerto Morelos, Mexico, 2021.
53. Braun-Blanquet, J. *Plant Sociology: The Study of Plant Communities*, 1st ed.; McGraw-Hill: New York, NY, USA, 1932.
54. Otsu, N. A Tlreshold Selection Method from Gray-Level Histograms. *IEEE Trans. Syst. Man. Cybern.* **1979**, *9*, 62–66. [CrossRef]
55. Yamamuro, M.; Nishimura, K.; Kishimoto, K.; Nozaki, K.; Kato, K.; Negishi, A.; Otani, K.; Shimizu, H.; Hayashibara, T.; Sano, M.; et al. Mapping Tropical Seagrass Beds with an Underwater Remotely Operated Vehicle (ROV). In *Recent Advances in Marine Science and Technology*; Saxena, N., Ed.; Japan International Marine Science and Technology Federation: Yokosuka, Japan, 2002; pp. 177–181.
56. De Almeida, L.R.; Ávila-Mosqueda, S.V.; Silva, R.; Mendoza, E.; van Tussenbroek, B.I. Monitoring Seagrass Meadows Using Satellite Images: Possible Uses, Limitations and Challenges. In Proceedings of the 3rd International Congress on Marine Energy CEMIE-Océano, Puerto Morelos, Quintana Roo, Mexico, 5–7 September 2023; Chávez, V., Ed.; pp. 71–72.
57. Lyzenga, D.R. Passive Remote Sensing Techniques for Mapping Water Depth and Bottom Features. *Appl. Opt.* **1978**, *17*, 379. [CrossRef] [PubMed]
58. CONABIO/UNAM Cobertura Bentónica de Los Ecosistemas Marinos Del Caribe Mexicano: Cabo Catoche—Xcalak. 2018. Available online: http://www.conabio.gob.mx/informacion/metadata/gis/covertv2gw.xml?_httpcache=yes&_xsl=/db/metadata/xsl/fgdc_html.xsl&_indent=no (accessed on 4 February 2021).
59. Cerdeira-Estrada, S.; Martell-Dubois, R.; Heege, T.; Rosique-De La Cruz, L.O.; Blanchon, P.; Ohlendorf, S.; Müller, A.; Silva-Casarín, R.; Mariño-Tapia, I.J.; Martínez-Clorio, M.I.; et al. Batimetría de Los Ecosistema Marinos Del Caribe Mexicano: Cabo Catoche—Xcalak. *Catálogo metadatos geográficos. Com. Nac. para el Conoc. y Uso la Biodivers*. 2018. Available online: http://www.conabio.gob.mx/informacion/gis/?vns=gis_root/biodiv/bidarrecif/batimv2gw (accessed on 10 September 2021).
60. Wentworth, C.K. A Scale of Grade and Class Terms for Clastic Sediments. *J. Geol.* **1922**, *30*, 377–392. [CrossRef]
61. Sherman, D.J.; Bauer, B.O. Dynamics of Beach-Dune Systems. *Prog. Phys. Geogr.* **1993**, *17*, 413–447. [CrossRef]
62. CONANP/PROCODES Informe Final Del Diagnóstico Del Estado de Conservación y de La Vegetación de La Duna Del Área de Influencia Del Parque Nacional Arrecifes de Puerto Morelos. *Technical Study*. 2017. Available online: https://www.gob.mx/conanp/archivo/documentos?order=DESC&page=31 (accessed on 21 September 2020).
63. Pellón, E.; de Almeida, L.R.; González, M.; Medina, R. Relationship between Foredune Profile Morphology and Aeolian and Marine Dynamics: A Conceptual Model. *Geomorphology* **2020**, *351*, 106984. [CrossRef]
64. Dean, R.G. Equilibrium Beach Profiles: Characteristics and Applications. *J. Coast. Res.* **1991**, *7*, 53–84.
65. Díez, J.; Uriarte, A.; Medina, R. A Parametric Model for the Dry Beach Equilibrium Profile. *J. Coast. Res.* 2017; *in press*.
66. Labarthe, C.; Castelle, B.; Marieu, V.; Garlan, T.; Bujan, S. Observation and Modeling of the Equilibrium Slope Response of a High-Energy Meso-Macrotidal Sandy Beach. *J. Mar. Sci. Eng.* **2023**, *11*, 584. [CrossRef]
67. Alcérreca-Huerta, J.C.; Cruz-Ramírez, C.J.; de Almeida, L.R.; Chávez, V.; Silva, R. Interconnections between Coastal Sediments, Hydrodynamics, and Ecosystem Profiles on the Mexican Caribbean Coast. *Land* **2022**, *11*, 524. [CrossRef]
68. Guzmán, O.; Mendoza, E.; van Tussenbroek, B.I.; Silva, R. Effects of Climate-Change-Related Phenomena on Coastal Ecosystems in the Mexican Caribbean. *Sustainability* **2023**, *15*, 12042. [CrossRef]
69. Perera-Valderrama, S.; Cerdeira-Estrada, S.; Martell-Dubois, R.; Rosique-de la Cruz, L.; Caballero-Aragón, H.; Valdez-Chavarin, J.; López-Perea, J.; Ressl, R. A New Long-Term Marine Biodiversity Monitoring Program for the Knowledge and Management in Marine Protected Areas of the Mexican Caribbean. *Sustainability* **2020**, *12*, 7814. [CrossRef]
70. Anfuso, G.; Postacchini, M.; Di Luccio, D.; Benassai, G. Coastal Sensitivity/Vulnerability Characterization and Adaptation Strategies: A Review. *J. Mar. Sci. Eng.* **2021**, *9*, 72. [CrossRef]
71. Narayan, S.; Beck, M.W.; Reguero, B.G.; Losada, I.J.; van Wesenbeeck, B.; Pontee, N.; Sanchirico, J.N.; Ingram, J.C.; Lange, G.-M.; Burks-Copes, K.A. The Effectiveness, Costs and Coastal Protection Benefits of Natural and Nature-Based Defences. *PLoS ONE* **2016**, *11*, e0154735. [CrossRef] [PubMed]
72. Temmerman, S.; Meire, P.; Bouma, T.J.; Herman, P.M.J.; Ysebaert, T.; De Vriend, H.J. Ecosystem-Based Coastal Defence in the Face of Global Change. *Nature* **2013**, *504*, 79–83. [CrossRef] [PubMed]
73. Planet Team Planet Application Program Interface: In Space for Life on Earth. Available online: https://api.planet.com (accessed on 14 May 2022).